Biophysics and Physicobiology

Regular Article

Structure-function relationship of KaiC around dawn

Yoshihiko Furuike[1,2], Eiki Yamashita[3], Shuji Akiyama[1,2]

[1] *Research Center of Integrative Molecular Systems (CIMoS), Institute for Molecular Science, National Institutes of Natural Sciences, Okazaki, Aichi 444-8585, Japan*
[2] *Molecular Science Program, Graduate Institute for Advanced Studies, SOKENDAI, Okazaki, Aichi 444-8585, Japan*
[3] *Institute for Protein Research, Osaka University, Suita 565-0871, Japan*

KaiC is a multifunctional enzyme functioning as the core of the circadian clock system in cyanobacteria: its N-terminal domain has adenosine triphosphatase (ATPase) activity, and its C-terminal domain has autokinase and autophosphatase activities targeting own S431 and T432. The coordination of these multiple biochemical activities is the molecular basis for robust circadian rhythmicity. Therefore, much effort has been devoted to elucidating the cooperative relationship between the two domains. However, structural and functional relationships between the two domains remain unclear especially with respect to the dawn phase, at which KaiC relieves its nocturnal history through autodephosphorylation. In this study, we attempted to design a double mutation of S431 and T432 that can capture KaiC as a fully dephosphorylated form with minimal impacts on its structure and function, and investigated the cooperative relationship between the two domains in the night to morning phases from many perspectives. The results revealed that both domains cooperate at the dawn phase through salt bridges formed between the domains, thereby non-locally co-activating two events, ATPase de-inhibition and S431 dephosphorylation. Our further analysis using existing crystal structures of KaiC suggests that the states of both domains are not always in one-to-one correspondence at every phase of the circadian cycle, and their coupling is affected by the interactions with KaiA or adjacent subunits within a KaiC hexamer.

◄ *Significance* ►

In both prokaryotes and eukaryotes, the night history of the circadian clock system is reset by disassembly of highly stabilized complexes of clock proteins. In cyanobacteria, the clock protein KaiC coordinates own ATPase, kinase, and phosphatase activities in the pre- to post-dawn phases to promote the initiation of the next cycle. In this study, we investigated crystal structures of KaiC and its mutants and revealed the structural basis for the phase-dependent coordination of the multiple activities residing in two distinct domains.

Introduction

Cyanobacteria adapt to the environmental day/night cycle using approximately 24 h rhythms generated by circadian clock system [1,2]. The circadian rhythm is completely self-sustained as it persists even without any external cues [3]. Its period length is kept nearly 24 h over a physiological range of temperature through a yet fully unresolved mechanism to compensate for temperature changes [4-6]. Cyanobacterial clock achieves phase entrainment at the cellular [7] and

Corresponding author: Shuji Akiyama, Research Center of Integrative Molecular Systems (CIMoS), Institute for Molecular Science, National Institutes of Natural Sciences, 38 Nishigo-Naka, Myodaiji, Okazaki, Aichi 444-8585, Japan. ORCID iD: https://orcid.org/0000-0002-7184-189X, e-mail: akiyamas@ims.ac.jp

molecular scales [8,9] by shifting their phase back and forth in response to stimuli from the day/night environmental cycles. *In vitro* reconstruction of a minimal oscillator [10,11], which satisfies the above unique properties of self-sustainment, temperature compensation, and synchronization, provides practical means to study detailed mechanisms of the circadian clock system in cyanobacteria [3,12].

The *in vitro* clock oscillator of the cyanobacterium *Synechococcus elongatus* PCC 7942 can be reconstructed by mixing three kinds of clock proteins called KaiA, KaiB, and KaiC in the presence of adenosine triphosphate (ATP) [10]. KaiC is composed of tandemly duplicated N-terminal (CI) and C-terminal (CII) domains [13], and forms a hexamer by incorporating one molecule of ATP or adenosinde diphosphate (ADP) at every CI-CI and CII-CII interface (Figure 1A). KaiA binds a C-terminal tail of KaiC and promotes autophosphorylation at dual phosphorylation sites, S431 and T432, in the CII domain [14,15]. On the other hand, KaiB binds the CI domain and antagonizes the effect of KaiA by sequestering KaiA further onto KaiB [16,17]. In the presence of KaiA and KaiB, the dual phosphorylation sites undergo circadian phosphorylation/dephosphorylation in the following order [18,19]; ST → SpT → pSpT → pST → ST, where S, T, pS, and pT represent dephosphorylated S431, dephosphorylated T432, phosphorylated S431, and phosphorylated T432, respectively.

At the same time, adenosine triphosphatase (ATPase) activity in the CI domain is robustly activated and then inactivated with the period of 24 h in the presence of KaiA and KaiB [4]. Much attention has been focused on the ATPase activity of KaiC, because the period length of the KaiC phosphorylation cycle is inversely correlated to the ATPase activity of KaiC alone [4]. Furthermore, the low ATPase activity of ~12 ATP d^{-1} is one of the origins of clock slowness in cyanobacteria [20], and its temperature insensitivity is also considered as one of the origins of the system-level temperature compensation [5]. Exploring the molecular basis for the crosstalk between CI-ATPase [4,20] and CII-autokinase/autophosphatase [18,19] is of particular importance for understanding the core clock oscillator in cyanobacteria.

In the previous study [21,22], we reported a series of X-ray crystal structures that nearly cover the major states constituting the KaiC phosphorylation cycle (Table 1). A motif identified as phosphor-switch (PSw) in the CII domain, which corresponds to 14 residues (T416–H429) upstream of the dual phosphorylation sites, forms a short α-helix in the ST and SpT states and a coiled structure in the pSpT and pST states (Figure 1B). The helix-to-coil transition of the PSw in the CII domain is allosterically coupled to the CI domain in the manner of nucleotide exchange [21] and regulatory state of ATPase [22], through a salt bridge in the E214–R217–Q394 (ERQ) triad at the boundary between the CI and CII domains (Figure 1B). The regulatory status of CI-ATPase is further linked to the intermolecular interaction between KaiB and KaiC. A ratio (*b*-value) of the CI-ATPase activity in full-length KaiC to that in the corresponding CI fragment serves one measure of this linkage, correlating inversely to the affinity of KaiC for KaiB [22]. During the circadian cycle, the relationship of above five factors (KaiB affinity, CI-ATPase, ERQ triad, PSw, and phosphoryl modification) is considered to fluctuate rhythmically from phase to phase [21-24].

In order to investigate the CI-CII crosstalk, attempts have been made to fix KaiC in a specific state by introducing amino acid substitutions to the dual phosphorylation sites. For phosphorylated KaiC, a suitable set of phosphomimetic mutations were found at a relatively early stage [4,18]; S431D/T432E (KaiC-DE) or S431E/T432E (KaiC-EE) substitutions to mimic KaiC-pSpT. On the other hand, S431A/T432A (KaiC-AA) substitutions have been used for about two decades as a potential mimic of the fully dephosphorylated state [25], KaiC-ST. Our recent study in terms of the above five factors [22], however, clearly indicated that KaiC-AA is structurally and functionally distinct from KaiC-ST, but rather mimics KaiC-ST activated by KaiA binding. A marked reduction in the side chain volume due to the dual alanine substitutions is the main cause of these structural and functional mismatches, preventing the study of the CI-CII crosstalk especially at dawn, when KaiC-ST transiently accumulates to reset nocturnal history and restart the next circadian cycle.

In our previous study [24], the dual phosphorylated sites were replaced by a set of non-phosphorylatable amino acids with appropriate side chain volumes. T432 was mutated to valine (T432V), as both its side chain volume and topology are most similar to those of threonine (Figure 1C) and KaiC-SV is known to share the helical PSw with KaiC-ST [21]. In addition to the T432V replacement, S431 was mutated to cysteine (S431C) as both its side chain volume and topology are closest to those of serine (Figure 1C). Cysteine is rarely phosphorylated under physiological conditions [26], and we confirmed that this is also the case for KaiC [21]. Trp fluorescence spectroscopy implied the potential of KaiC-CV as a KaiC-ST mimetic [22,24], but it has not been evaluated in terms of its ATPase activity or structure at atomic resolution.

In this study, the structure and function of KaiC-CV were studied in terms of the above five factors. We found that the helical conformation of the PSw is marginally stabilized by a set of delicate non-bonded interactions, which are sensitive even to a 0.3 Å increase in the van der Waals (vdW) radius at the γ position of the side chain upon the S431C substitution. The helical PSw was destabilized also in another mutant, KaiC-TV, with a further increase in volume at the 431st position. At the same time, the regulatory status of CI-ATPase in KaiC-CV with the non-helical PSw was essentially similar to that in KaiC-ST with the helical PSw. Taken together, KaiC-CV and KaiC-TV are potential mimics of intermediate states just before KaiC-ST is formed at dawn, in which CI-ATPase and PSw are weakly coupled. We further analyzed the correspondence of the five factors for a series of other phosphomimetic mutants. The structural and functional factors reflecting the CI-CII crosstalk are not always in one-to-one correspondence throughout the circadian cycle and likely change in a less coupled manner at particular phases.
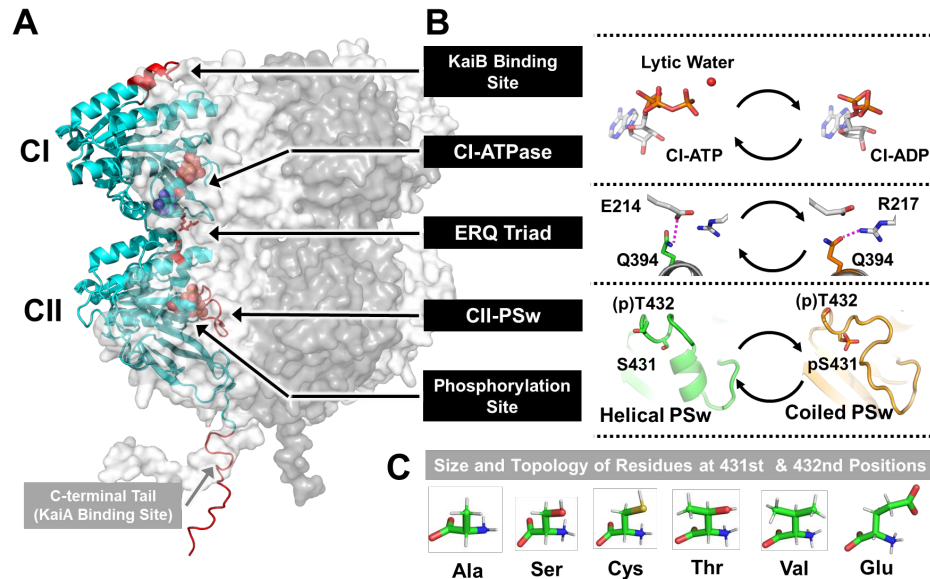
Figure 1 Overview of CI-CII crosstalk in KaiC. (A) Five structural and functional factors mapped on the crystal structure of the KaiC hexamer [13]. A representative KaiC monomer is highlighted using ribbon model. (B) Key factors [21,22] essential for the CI-CII crosstalk. (C) Comparison of size and topology of amino acids utilized for S431/T432 substitutions to mimic the dephosphorylated and phosphorylated states of KaiC.

Table 1 KaiC crystal structure library consisting of new crystal structures reported in this study and existing crystal structures reported in our previous studies [21,22].

	1	2	3	4	5
Reference Number	[21]	[22]	[21]	[21]	This Study
PDB ID	7DXQ	7DY1	7V3X	7DY2	8WV8
Resolution (Å)	2.80	2.20	3.10	3.04	2.93
Space Group	$P2_12_12_1$	$P2_12_12_1$	$P2_1$	$P2_1$	$P6_3$
Number of KaiC in Asymm. Unit	6 KaiC	6 Te-KaiC[a]	24 KaiC	12 KaiC	2 KaiC
Oligomerization	1 Hexamer	1 Hexamer	4 Hexamer	2 Hexamer	Dimer in Hexamer
CI-Nucleotide	6 ATP	6 ATP	23 ATP + 1 ADP	3 ATP + 9 ADP	2 ATP
Phosphorylation Site	6 pSpT	6 pSpT + 1 pST	11 pSpT + 13 pST	11 pST + 1 ST	2 CV

	6	7	8	9	10
Reference Number	This Study	[21]	[21]	[21]	[22]
PDB ID	8WVE	7DYK	7DYJ	7DYI	7DYE
Resolution (Å)	2.73	2.99	2.40	2.64	2.60
Space Group	$P6_3$	$P6_3$	$P6_3$	$P6_3$	$R3$
Number of KaiC in Asymm. Unit	2 KaiC	2 KaiC	2 KaiC	2 KaiC	2 KaiC
Oligomerization	Dimer in Hexamer	Dimer in Hexamer	Dimer in Hexamer	Dimer in Hexamer	Dimer in Hexamer
CI-Nucleotide	2 ATP	2 ATP	2 ATP	2 ATP	2 ATP
Phosphorylation Site	2 TV	2 SV	2 ST	2 SE	2AA

[a] KaiC homologue from *Themosynecococcus elongatus*.

Materials and Methods

Expression and Purification of Kai Proteins

KaiC-CV and KaiC-TV were expressed in *Escherichia coli* BL21(DE3) as described previously [25] and were purified with affinity chromatography using glutathione S-transferase tag, gel-filtration chromatography using Sephacryl S300 (Cytiva), and ion-exchange chromatography using Resource Q (Cytiva) as reported previously [18,27].

Biochemical Assays

The ATPase activity and the phosphorylation states of KaiC were measured at 30 °C as previously described [27,28]. To estimate *b*-values [22], the ATPase activities of a full-length KaiC, a full-length KaiC with E318Q substitution to inactivate ATP consumptions in the CII domain, and a CI fragment were measured. The affinity of KaiB for KaiC was evaluated as previously reported [22]. KaiB (0.06 mg/mL) was incubated with KaiC at 30 °C for 30 h. Aliquots were taken and then subjected to native polyacrylamide gel electrophoresis analysis.

Crystallization and X-ray Diffraction

KaiC-CV and KaiC-TV were crystallized by the vapor diffusion method as reported previously [21,24]. Preliminary X-ray diffraction experiments were conducted using FRX-Synergy (RIGAKU). Final data sets were collected on beamline BL44XU at SPring-8 (Harima, Japan). X-ray at the wavelength of 0.9 Å was radiated against KaiC crystals frozen under a cryostream at 100 K. Diffraction images were recorded by using EIGER X 16M (DECTRIS), XDSGUI [29], and KAMO, semi-automatic data processing system implemented in SPring-8 [30]. The diffraction data were processed by molecular replacement method using MOLREP [31] and 7DYJ [21] as a template. The model structures were refined by Refmac5 [32] with free-R flags transferred from 7DYJ. The model buildings were conducted with COOT [33]. Graphic representations were generated using PyMOL (Schrödinger). The crystallographic statistics were listed in Table 2.

Analysis of ERQ Triad in KaiC Crystal Structure Library

Structures of the ERQ triads were carefully investigated according to the following procedure. We selected all crystallographically independent ERQ triads from our crystal structure library (Table 1). A Fo-Fc omit map was generated for each of the independent ERQ triads to confirm the reliability of each triad model. Among 60 triads tested, 44 triads exhibiting consistency between the omit map and the model structure were subjected to geometric analysis.

Table 2 Statistics of X-ray diffraction experiments, refinements, and model buildings for KaiC-CV and KaiC-TV.

Protein	KaiC-CV	KaiC-TV
Data Collection		
Space group	$P6_3$	$P6_3$
Unit cell parameters		
a, b, c (Å)	95.2, 95.2, 184.1	94.2, 94.2, 179.2
α, β, γ (°)	90, 90, 120	90, 90, 120
Wavelength (Å)	0.9	0.9
Resolution range (Å)[a]	49.2-2.93	48.2-2.73
	(3.03-2.93)	(2.83-2.73)
Total reflections	209178	254691
Unique reflections	20257 (1985)	23865 (2321)
Redundancy	10.3 (10.8)	10.7 (11.0)
Completeness (%)	99.7 (98.1)	99.8 (98.0)
R_{merge} (%)[b]	11.7 (>100)	9.2 (91.8)
(I)/sigma(I)	15.8 (2.4)	14.9 (2.5)
Model building		
Molecular replacement	7DYJ	7DYJ
Total atoms	6654	6563
Protien	6510	6407
Ligands	128	128
Water	16	28
R_{work} (%)[c]	27.6	28.0
R_{free} (%)[c]	33.5	33.8
R.M.S.D. from ideality		
Bond length (Å)	0.002	0.002
Bond angles (°)	1.2	0.7
Average B factors (Å^2)	82.5	72.8
Rmachandran plot		
Most favored (%)	82.6	85.8
Allowed (%)	17.0	14.2
Disallowed (%)	0.4	0.0
PDB code	8WV8	8WVE

[a]Values in parentheses are for the highest-resolution shell.
[b]$R_{merge} = \Sigma|I-<I>|/\Sigma I$, where I correspond to the observed intensity of reflections.
[c]$R_{work, free}=\Sigma|F_{obs}|-|F_{calc}|/\Sigma|F_{obs}|$. R_{free} is the cross-validation of R-factor using the test reflections, 5% of the data, not included in the refinements.

Results and Discussion

KaiC-CV with Non-helical PSw

Our previous study [21] has shown that the PSw folds into the helical conformation in both KaiC-ST and KaiC-SV (Figure 2A). Note that in the figures and tables below, previously reported data are marked with an asterisk (like ST* in Figure 2A) to clearly distinguish between data newly reported in this paper and the data we have previously reported [21,22]. As shown in Figure 2B, the hydroxyl group of S431 is involved in multiple hydrogen bonds with a recruited water molecule (W in Figure 2B) and carbonyl oxygen atoms of I425 and S428, eventually stably capping the C-terminus of the helical PSw. To prevent slow but reversible phosphorylation of S431 in KaiC-SV [21], S431 was replaced with cysteine, which is known to possess a similar volume and topology of side chains as serine (Figure 1C), an ability to engage an atom at the γ-position in hydrogen bond formation, and is hardly phosphorylated [21].
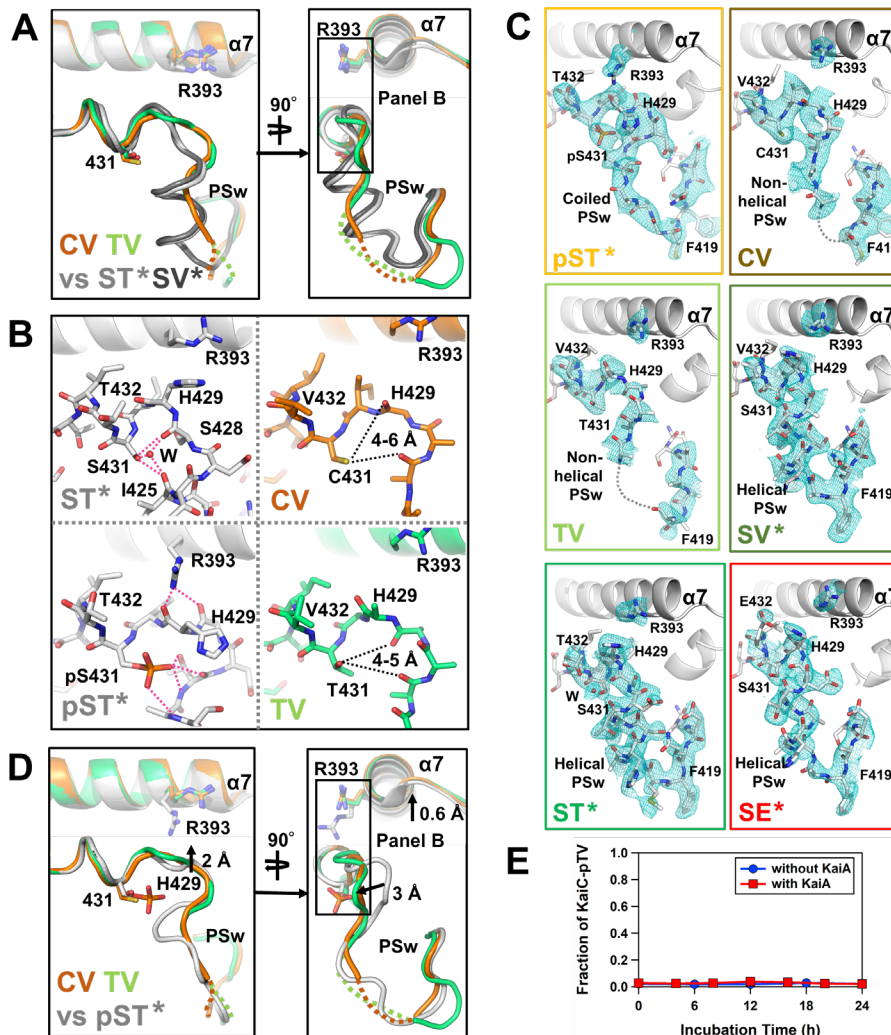
Figure 2 Structures of phospho-switch (PSw). The structures labeled with asterisks are regenerated using coordinates (Table 1) reported in the previous studies [21,22]. (A) Comparison of the 431st position, the PSw, R393, and α7 helix among KaiC-CV (orange), KaiC-TV (light green), KaiC-ST (white), and KaiC-SV (gray). (B) Zoomed-in-view of the boxed regions in panel (A) and (D). Interatomic distances beyond hydrogen-bond distances (3.5 Å) are indicated by black dotted lines. The potential hydrogen bonds are highlighted by magenta dotted lines. (C) Fo-Fc omit maps (cyan mesh at 2.0 σ level) as evidences of coiled PSw in KaiC-pST, non-helical PSws in KaiC-CV and KaiC-TV, and helical PSws in KaiC-SV, KaiC-ST, and KaiC-SE. The α7 helix harbors R393 and Q394. (D) Comparison among KaiC-CV, KaiC-TV, and KaiC-pST (white). (E) Complete inhibition of auto-phosphorylation activity in KaiC-TV.

   The crystal of KaiC-CV belonged to the same space group ($P6_3$) as KaiC-ST and KaiC-SV [21], and diffracted to 2.9 Å resolution (Table 2). KaiC-CV formed a hexamer as KaiC-ST and KaiC-SV, every subunit of which bound one ATP molecule to each of the CI and CII domains (Table 1). Contrary to our design based on the careful diagnosis of the existing crystal structures, KaiC-CV was crystallized in a form containing a non-helical PSw (Figure 2A and 2C). The S_γ atom of C431 was in 4-6 Å interatomic distance from the surrounding residues, and did not form any non-covalent interactions that assisted the capping of the helical PSw seen in KaiC-ST and KaiC-SV (Figure 2B). Consequently, the PSw of KaiC-CV became less compact than KaiC-ST (Figure 2A). The present result illustrates how elaborately the hydrogen bond network has been designed to stabilize the C-terminal capping of the helical PSw, as the vdW radius of the O_γ atom of S431 differs from that of the S_γ atom of C431 by only 0.3 Å (Figure 2A and 2B).

   The PSw of KaiC-CV formed a structure that simply could not be classified as either helical or coiled. Compared to KaiC-pST (Figure 2D), the absence of the phosphoryl modification in KaiC-CV resulted in the reduction of the cavity around the 431st position, bringing the main chain of PSw in KaiC-CV closer to the thiol group of C431 by approximately 3 Å. An accurate position of the side chain of H429 could not be assigned in KaiC-CV possibly due to enhanced flexibility (Figure 2C). To be consistent with this interpretation, a hydrogen bond between R393 and the main chain of H429 formed in KaiC-pST was disrupted in KaiC-CV (Figure 2B) and thereby the side chain of R393 from the neighboring helix (α7) was flipped toward the CI side (Figure 2D). The main chain of H429 also shifted 2-3 Å toward the CI domain (Figure 2D), and consequently the α7 helix moved 0.6 Å in the CI direction. The PSw in KaiC-CV was found to be non-helical form, in-between the helical structure like KaiC-ST and the coiled structure like KaiC-pST (Figure 2A and 2D).

KaiC-CV and KaiC-TV as Intermediate States before KaiC-ST Formation

   The PSw of KaiC-CV was in the non-helical form (Figure 2A), but was distinct from the coiled conformation (Figure 2D) identified in KaiC-pSpT and KaiC-pST with lower CI-ATPase activity [4,22]. To investigate any allosteric effects of the non-helical PSw, we measured the steady-state ATPase activity of KaiC-CV at 30°C and compared it with those of other KaiC mutants (Figure 3A). The ATPase activity of KaiC-CV was 12.0 ± 1.4 ATP d^{-1}. It was much higher than those of phosphomimetic variants of KaiC-pSpT (KaiC-EE) and KaiC-pST (KaiC-EV) with the coiled PSw, but still slightly smaller than those of KaiC-ST and KaiC-SV. A similar trend was observed also for the b-value (Figure 3B). The down-regulation of CI-ATPase confirmed in KaiC-EE and KaiC-EV is partially canceled in KaiC-CV.

   The effect of the limited down-regulation was investigated in terms of the KaiB affinity. KaiC and its mutants were incubated with the equal amount of KaiB at 30°C for 30 h and then subjected to the densitometric analyses [22]. The normalized KaiB affinities of KaiC-ST and KaiC-CV were approximately 50 and 90%, respectively, of that of KaiC-EV (Figure 3C). In terms of the b-value and the KaiB affinity, it seems reasonable to consider that KaiC-CV retains functional properties in-between those of KaiC-pST and KaiC-ST.

   To confirm the suggested sensitivity to the volume increase around the γ position of S431, we prepared a KaiC-TV mutant that is never phosphorylated irrespective of the presence of KaiA (Figure 2E). The PSw of KaiC-TV adopted a non-helical configuration as was observed for KaiC-CV (Figure 2A, 2C, and 2D). Nevertheless, its b-value and KaiB affinity were similar to those of KaiC-ST (Figure 3B and 3C), suggesting the CI domain of KaiC-TV in the same regulatory state as KaiC-ST. KaiC-TV is functionally closer to KaiC-ST than KaiC-CV (Figure 3), but structurally KaiC-
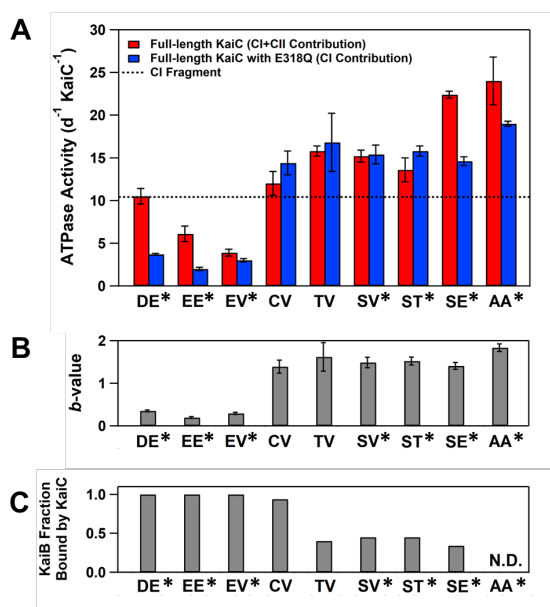
Figure 3 Regulatory status of CI-ATPase. The data labeled with asterisks are taken from our previous study [22]. (A) Steady-state ATPase activities of wild-type KaiC (KaiC-ST) and phospho-mimicking mutants. Red and blue bars correspond to activities of full-length KaiC (contribution from CI and CII) and full-length KaiC with E318Q substitution (contribution only from CI), respectively. A dotted line indicates the activity of CI fragment without mutations. The blue bar below/beyond the dotted line indicates that the CI-ATPase of the mutant is down/up-regulated through CI-CII crosstalk. (B) b-values calculated as ratios of blue bars to the dotted line in panel (A). (C) KaiB-KaiC affinity evaluated by estimating KaiB fraction bound by KaiC.

TV shares the non-helical PSw (Figure 2A) with KaiC-CV. In this sense, both KaiC-TV and KaiC-CV are considered to be intermediate states on going from the pST to ST states just before forming the helical PSw.

Variation of ERQ Triad

In the previous study [21], we demonstrated that Q394 switches the hydrogen-bonding partner from R217 to E214 on going from the pST to ST states (Figure 1B). To further test our interpretation of KaiC-CV and KaiC-TV, we conducted systematic analysis of the ERQ triads (Figure 4A) using our KaiC crystal structure library including KaiC-CV and KaiC-TV (Table 1). The ERQ triads are categorized into four groups (Figure 4B); Q394 hydrogen-bonds solely to R217 (R-biased triad), Q394 hydrogen-bonds to both E214 and R217 (balanced triad), Q394 hydrogen-bonds solely to E214 (E-biased triad), and Q394 hydrogen-bonds neither R217 and E214 (free triad).

In KaiC-pSpT, the R-biased and balanced triads accounted for the majority (Figure 4A), and their ratios were nearly identical (Figure 4B). The fraction of the R-biased triad is maximized upon transitioning from KaiC-pSpT to KaiC-pST. This was especially the case for the pST subunit that binds ADP in the CI domain (Figure 4B) [21]. By contrast, as demonstrated in our previous study [21], the triads are mostly switched to the E-biased form on going from the pST to ST states. One exception to this switching was identified in a KaiC hexamer, which contains one ST and five pST subunits [PDB ID: 7DY2], suggesting that the effect of adjacent subunits within the hexamer cannot be ignored. This switching during the transition from the pST to ST states accompanies a sliding of the CI-CI interface [21] and assists to cancel the down-regulation of CI-ATPase [22].

The triads in KaiC-CV were yet R-biased (Figure 4A), while those of KaiC-TV were E-biased or free as were observed for KaiC-SV (Figure 4B). These observations support our interpretation of KaiC-TV being closer to KaiC-ST and KaiC-SV than to KaiC-CV. The triads of KaiC-AA, the KaiA-activated mimic of KaiC with the coiled PSw [22], were R-biased or free and evidently distinct from KaiC-ST with the helical PSw. On the other hand, a KaiC-SpT–mimicking mutant (KaiC-SE) revealed the R-biased triads despite of its helical PSw (Figure 2C) [21]. It must be noted that a variety of the ERQ triads are not simply due to crystal packing effects, because all of the crystals for KaiC-CV, KaiC-TV, KaiC-SV, KaiC-ST, and KaiC-SE belonged to the same space group of $P6_3$ (Table 1). The present results implies that the structures of the ERQ triad and PSw are not always in full correspondence with each other. Their coupling can become weaker at certain phases especially when activated (KaiC-AA) or phosphorylated by KaiA (KaiC-SE), and in addition diversity can emerge under the influence of adjacent subunits within the hexamer.

Phase to Phase Diversity of CI-CII Crosstalk

Figure 5 and 6 summarizes our past [21,22] and current observations for the five factors during the circadian cycle. In KaiC-pSpT, every CI-CI interface is slightly shifted by ~1 Å (Figure 5A and 5D) away from the CII side to down-regulate the CI-ATPase activity (↓ in Figure 6) [22]. The affinity of KaiC-pSpT for KaiB is highest among the states examined so far as evidenced by its lowest b-value [22] (Figure 3B). The ERQ triad is essentially R-biased or balanced (Figure 4B) and the PSw adopts the coiled conformation [21]. These properties of the pSpT state are essentially inherited by the pST state (Figure 5A, 5B, and 5C), except that the R-biased form predominates in the pST subunit with ADP in its CI domain (Figure 4B).

In KaiC-CV, the slide of the CI-CI interface is no longer obvious (Figure 5D), and probably associated with it, the down-regulation of the CI-ATPase is largely canceled (↓↑ in Figure 6). One possible reason why the KaiB affinity of KaiC-CV is still high despite the increase in the b-value (Figure 3B and 3C) may be its R-biased triad as the pST state (Figure 6). The 0.3 Å increase in vdW radius of the γ atom at the 431st position is the sufficient perturbation to turn the PSw morphology to non-helical (Figure 2A), but not enough to induce the coiled PSw seen in the pST and pSpT states (Figure 2D).

KaiC-TV mimics well both the CI-CI interface (Figure 5D) and the CI-ATPase activity (Figure 3A) in the fully dephosphorylated states. The same applies to the b-value and the KaiB affinity (Figure 3B and 3C). The ERQ triad of KaiC-TV is E-biased as confirmed for KaiC-SV and KaiC-ST (Figure 4B). The local structure of the PSw in KaiC-TV is classified as non-helical like KaiC-CV (Figure 2D and 6), but the quaternary structure of KaiC-TV is rather similar to KaiC-SV and KaiC-ST than KaiC-CV, as the CII domain gets closer to the CI side on going from KaiC-pST to KaiC-CV, and then to KaiC-TV (Figure 5B). KaiC-TV differs from KaiC-ST only in the local interactions to maintain the helical morphology of the PSw (Figure 6).

KaiC-SE retains the same CI-CI interface (Figure 5D) and CI-ATPase activity (Figure 3A) as the fully dephosphorylated state, which well explains the similarities of the b-value and KaiB affinity to KaiC-ST (Figure 3B and 3C) [22]. However, several structural differences are identified between KaiC-SE and KaiC-ST: KaiC-SE has the same helical PSw as KaiC-ST (Figure 2C), but its R-biased ERQ triad differs from that of KaiC-ST (Figure 4B). Furthermore, the CII domain of KaiC-SE is further away from the CI side than KaiC-ST, and is in approximately the same position as that of KaiC-CV (Figure 5B). In a sense of quaternarily similar but locally different structure, the relationship between KaiC-SE and KaiC-CV is somewhat analogous to that between KaiC-TV and KaiC-ST (Figure 6).
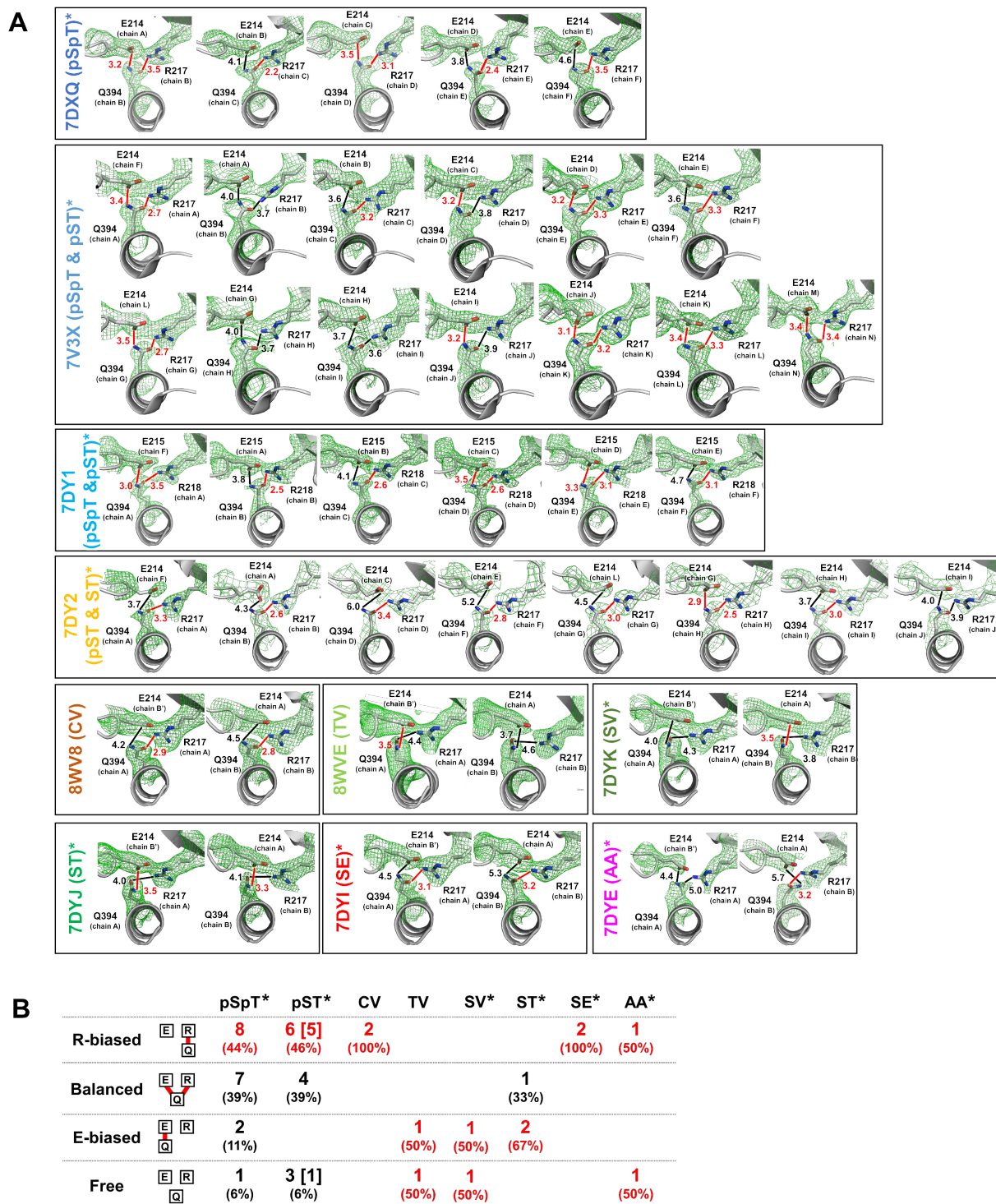
Figure 4 Structural classification of salt bridges found in the E214–R217–Q394 (ERQ) triad located at CI-CII and CI-CI interfaces. The structures labeled with asterisks are regenerated using coordinates (Table 1) reported in the previous studies [21,22]. (A) Crystallographically independent ERQ triads showing consistency between Fo-Fc omit maps (green mesh, 1.5 σ level) and model structures in the crystal structure library (Table 1). Interatomic distances beyond hydrogen-bond distances (3.5 Å) are indicated by black thick lines. The potential hydrogen bonds are highlighted by red thick lines. (B) Distribution of the ERQ triad structures in four major categories: R-biased (one hydrogen bond for R217-Q394 pair), balanced (one hydrogen bond for each of R217-Q394 and E214-Q394 pair), E-biased (one hydrogen bond for E214-Q394 pair) and free (no hydrogen bonds). Shown are the numbers of the ERQ triads found, with appearance frequencies in parenthesis. A value in square brackets corresponds to the number of the subunits binding CI-ADP [PDB ID: 7DY2].

In KaiC-AA, the KaiA-activated form of KaiC-ST, every CI-CI interface is shifted by ~1 Å (Figure 5A and 5D) to the CII side to up-regulate the CI-ATPase activity (↑ in Figure 6) [22]. As expected from the high b-value [22] (Figure 4B), KaiC-AA can no longer bind KaiB [22] (hyphen in Figure 6). The ERQ triad is R-biased or free (Figure 4).

As summarized in Figure 6, KaiC-CV, KaiC-TV, KaiC-SV, KaiC-ST, and KaiC-SE share the same level of the CI-ATPase activity without the down-regulation. This implies that structural polymorphisms detected in their PSw and ERQ triads (Figure 2, 4, and 5) are not necessary and sufficient conditions to induce the release of the down-regulation of the CI-ATPase. Conversely, factors that are present in the pSpT and pST states but not in the above five states are critical. As our previous study [21] has shown, the slide of the CI-CI interface takes place only during the transition of the pST to ST states, in which the α_7 helix harboring Q394 is pushed up toward the CI side by the side chains of R393 and H429 upon the coil-to-helix transition of the PSw (Figure 2B and 5B). Although accurate positions of the side chain of H429 could not be identified in KaiC-CV and KaiC-TV due to their less stabilized PSw, all of KaiC-CV, KaiC-TV, KaiC-SV, KaiC-ST, and KaiC-SE revealed the flip of the side chains of R393 to the CI side (Figure 5C). Our previous mutational study [28] also suggested a critical role of R393 in the CI-CII crosstalk. Our current interpretation is that the R393-mediated shift of the $\alpha7$ helix is the necessary and sufficient condition for releasing the down-regulation of CI-ATPase, and that the PSw and ERQ triad have the ability to further stabilize the shift, but show structural polymorphism depending on the phase in the circadian cycle.
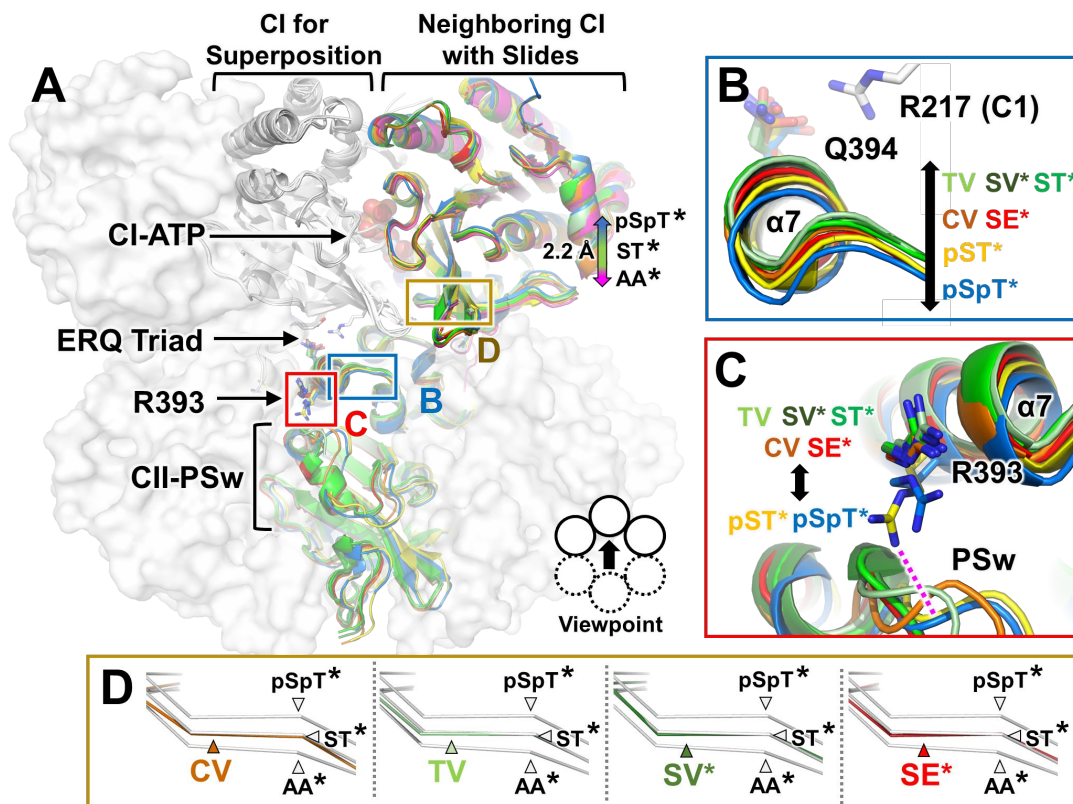
Figure 5 Structural crosstalk between CI and CII. The structures labeled with asterisks are regenerated using coordinates (Table 1) reported in the previous studies [21,22]. (A) Overview of three KaiC protomers viewed from an internal hole of KaiC hexamer. KaiC-pSpT (blue), KaiC-pST (yellow), KaiC-CV (orange), KaiC-TV (light green), KaiC-SV (dark green), KaiC-ST (green), KaiC-SE (red), and KaiC-AA (magenta) are superimposed using their CI domains drawn with white cartoon models. An ATP molecule (CI-ATP) is bound in the CI-CI interface. Sliding of the adjacent CI domains (colored) causes a change in the relative position of a lytic water molecule to CI-ATP (Figure 1B), resulting in the up/down-regulation of CI-ATPase [22]. (B) Gradual but obvious unidirectional shifts of the $\alpha7$ helix. (C) Orientation of the side chain of R393. The hydrogen bond between R393 and the main chains of the PSw in KaiC-pST is highlighted by a magenta dotted line. (D) Relative positions of the CI domains of KaiC mutants (colored). For visual clarity, the coloring is limited to only one mutant and the others are shown in white ribbon models.

Conclusion

The present examination supports that KaiC-CV and KaiC-TV mimic the possible intermediate states just prior to the formation of the ST state rather than the ST state itself: KaiC-pST → KaiC-CV → KaiC-TV → KaiC-ST. KaiC-SV will be the best ST-state mimetic currently known, except that it is very slowly phosphorylated in the presence of KaiA [21]. KaiC-TV is also a potential ST-state mimetic, except that its PSw is locally non-helical. KaiC is very delicately designed, and there seems to be no 431st mutations from natural amino acids that perfectly mimic the structure and function of fully dephosphorylated KaiC. This implies that we should be careful about blindly introducing numerous alanine substitutions to mammalian clock proteins with multiple phosphorylation sites.

Although our attempts of designing the perfect ST-state mimetic was not successful, the present study pointed out several important findings about the phase-to-phase variation of the CI-CII crosstalk during the circadian cycle. Although the PSw and ERQ triad exhibited structural polymorphism due to the effects of the cycle phase and adjacent subunits within the hexamer (Figure 2, 4, and 5), they as helical and E-biased forms have important roles in further supporting the R393-mediated shift of the α7 helix and then canceling the down-regulation of CI-ATPase, particularly during the transition from the pST to ST state (Figure 6).

Figure 6 Phase-to-phase variation of the CI-CII crosstalk emerging around dawn. Results shown include the data obtained in current and previous studies [21,22].

It must be noted that quaternarily similar but locally different structure between KaiC-CV and KaiC-SE does not explain the residual affinity of KaiC-CV for KaiB. This inconsistency implies that the conformational space of the KaiC hexamer is so diverse and the KaiB affinity is not explained solely by the logic of the *b*-value or KaiC crystal structures ever determined. In fact, the recent study using cryo-electron microscopy [34] identified a conformation of KaiC, in which the CI and CII domains come closer to each other than the crystal structures of KaiC. In order to resolve the numerous phenomena that cannot be rationally explained, it is necessary to continue to study the structure-function correlation of KaiC using various analytical methods.

Conflict of Interest

The authors declare that no competing interests exist.

Author Contributions

Y.F. and S.A. designed the research. Y.F. conducted biochemical experiments. Y.F. prepared KaiC crystals and collected diffraction data with supports from E.Y. S.A. and Y.F. wrote the paper with inputs from all the authors.

Data Availability

Acknowledgements

References

[1] Kondo, T., Strayer, C. A., Kulkarni, R. D., Taylor, W., Ishiura, M., Golden, S. S., et al. Circadian-rhythms in prokaryotes - luciferase as a reporter of circadian gene-expression in cyanobacteria. Proc. Natl. Acad. Sci. U.S.A. 90, 5672-5676 (1993). https://doi.org/10.1073/pnas.90.12.5672

[2] Ishiura, M., Kutsuna, S., Aoki, S., Iwasaki, H., Andersson, C. R., Tanabe, A., et al. Expression of a gene cluster as a circadian feedback process in cyanobacteria. Science 281, 1519-1523 (1998). https://doi.org/10.1126/science.281.5382.1519

[3] Partch, C. L. Orchestration of circadian timing by macromolecular protein assemblies. J. Mol. Biol. 432, 3426-3448 (2020). https://doi.org/10.1016/j.jmb.2019.12.046

[4] Terauchi, K., Kitayama, Y., Nishiwaki, T., Miwa, K., Murayama, Y., Oyama, T., et al. ATPase activity of KaiC determines the basic timing for circadian clock of cyanobacteria. Proc. Natl. Acad. Sci. U. S. A. 104, 16377-16381 (2007). https://doi.org/10.1073/pnas.0706292104

[5] Furuike, Y., Ouyang, D. Y., Tominaga, T., Matsuo, T., Mukaiyama, A., Kawakita, Y., et al. Cross-scale analysis of temperature compensation in the cyanobacterial circadian clock system. Commun. Phys. 5, 75 (2022). https://doi.org/10.1038/s42005-022-00852-z

[6] Sasai, M. Role of the reaction-structure coupling in temperature compensation of the KaiABC circadian rhythm. Plos Comput. Biol. 18, e1010494 (2022). https://doi.org/10.1371/journal.pcbi.1010494

[7] Fang, M. X., Chavan, A. G., LiWang, A., Golden, S. S. Synchronization of the circadian clock to the environment tracked in real time. Proc. Natl. Acad. Sci. U.S.A. 120, e2221453120 (2023). https://doi.org/10.1073/pnas.2221453120

[8] Yoshida, T., Murayama, Y., Ito, H., Kageyama, H., Kondo, T. Nonparametric entrainment of the in vitro circadian phosphorylation rhythm of cyanobacterial KaiC by temperature cycle. Proc. Natl. Acad. Sci. U.S.A. 106, 1648-1653 (2009). https://doi.org/10.1073/pnas.0806741106

[9] Ito, H., Kageyama, H., Mutsuda, M., Nakajima, M., Oyama, T., Kondo, T. Autonomous synchronization of the circadian KaiC phosphorylation rhythm. Nat. Struct. Mol. Biol. 14, 1084-1088 (2007). https://doi.org/10.1038/nsmb1312

[10] Nakajima, M., Imai, K., Ito, H., Nishiwaki, T., Murayama, Y., Iwasaki, H., et al. Reconstitution of circadian oscillation of cyanobacterial KaiC phosphorylation in vitro. Science 308, 414-415 (2005). https://doi.org/10.1126/science.1108451

[11] Tomita, J., Nakajima, M., Kondo, T., Iwasaki, H. No transcription-translation feedback in circadian rhythm of KaiC phosphorylation. Science 307, 251-254 (2005). https://doi.org/10.1126/science.1102540

[12] Akiyama, S. Structural and dynamic aspects of protein clocks: How can they be so slow and stable? Cell Mol. Life Sci. 69, 2147-2160 (2012). https://doi.org/10.1007/s00018-012-0919-3

[13] Pattanayek, R., Wang, J., Mori, T., Xu, Y., Johnson, C.H., Egli, M. Visualizing a circadian clock protein: Crystal structure of KaiC and functional insights. Mol. Cell 15, 375-388 (2004). https://doi.org/10.1016/j.molcel.2004.07.013

[14] Pattanayek, R., Williams, D. R., Pattanayek, S., Xu, Y., Mori, T., Johnson, C. H., et al. Analysis of KaiA-KaiC protein interactions in the cyano-bacterial circadian clock using hybrid structural methods. EMBO J. 25, 2017-2028 (2006). https://doi.org/10.1038/sj.emboj.7601086

[15] Vakonakis, I., LiWang, A. C. Structure of the C-terminal domain of the clock protein KaiA in complex with a KaiC-derived peptide: Implications for KaiC regulation. Proc. Natl. Acad. Sci. U.S.A. 101, 10925-10930 (2004). https://doi.org/10.1073/pnas.0403037101

[16] Snijder, J., Schuller, J. M., Wiegard, A., Lossl, P., Schmelling, N., Axmann, I. M., et al. Structures of the cyanobacterial circadian oscillator frozen in a fully assembled state. Science 355, 1181-1184 (2017).

https://doi.org/10.1126/science.aag3218

[17] Tseng, R., Goularte, N. F., Chavan, A., Luu, J., Cohen, S. E., Chang, Y. G., et al. Structural basis of the day-night transition in a bacterial circadian clock. Science 355, 1174-1180 (2017). https://doi.org/10.1126/science.aag2516

[18] Nishiwaki, T., Satomi, Y., Kitayama, Y., Terauchi, K., Kiyohara, R., Takao, T., et al. A sequential program of dual phosphorylation of KaiC as a basis for circadian rhythm in cyanobacteria. EMBO J. 26, 4029-4037 (2007). https://doi.org/10.1038/sj.emboj.7601832

[19] Rust, M. J., Markson, J. S., Lane, W. S., Fisher, D. S., O'Shea, E. K. Ordered phosphorylation governs oscillation of a three-protein circadian clock. Science 318, 809-812 (2007). https://doi.org/10.1126/science.1148596

[20] Abe, J., Hiyama, T. B., Mukaiyama, A., Son, S., Mori, T., Saito, S., et al. Atomic-scale origins of slowness in the cyanobacterial circadian clock. Science 349, 312-316 (2015). https://doi.org/10.1126/science.1261040

[21] Furuike, Y., Mukaiyama, A., Ouyang, D., Ito-Miwa, K., Simon, D., Yamashita, E., et al. Elucidation of master allostery essential for circadian clock oscillation in cyanobacteria. Sci. Adv. 8, eabm8990 (2022). https://doi.org/10.1126/sciadv.abm8990

[22] Furuike, Y., Mukaiyama, A., Koda, S. I., Simon, D., Ouyang, D., Ito-Miwa, K., et al. Regulation mechanisms of the dual ATPase in KaiC. Proc. Natl. Acad. Sci. U.S.A. 119, e2119627119 (2022). https://doi.org/10.1073/pnas.2119627119

[23] Simon, D., Mukaiyama, A., Furuike, Y., Akiyama, S. Slow and temperature-compensated autonomous disassembly of KaiB-KaiC complex. Biophys. Physicobiol. 19, e190008 (2022). https://doi.org/10.2142/biophysico.bppb-v19.0008

[24] Mukaiyama, A., Furuike, Y., Yamashita, E., Akiyama, S. Highly sensitive tryptophan fluorescence probe for detecting rhythmic conformational changes of KaiC in the cyanobacterial circadian clock system. Biochem. J. 479, 1505-1515 (2022). https://doi.org/10.1042/BCJ20210544

[25] Nishiwaki, T., Satomi, Y., Nakajima, M., Lee, C., Kiyohara, R., Kageyama, H., et al. Role of KaiC phosphorylation in the circadian clock system of Synechococcus elongatus PCC 7942. Proc. Natl. Acad. Sci. U.S.A. 101, 13927-13932 (2004). https://doi.org/10.1073/pnas.0403906101

[26] Buchowiecka, A. K. Puzzling over protein cysteine phosphorylation - assessment of proteomic tools for s-phosphorylation profiling. Analyst 139, 4118-4123 (2014). https://doi.org/10.1039/c4an00724g

[27] Ouyang, D., Furuike, Y., Mukaiyama, A., Ito-Miwa, K., Kondo, T., Akiyama, S. Development and optimization of expression, purification, and ATPase assay of kaiC for medium-throughput screening of circadian clock mutants in cyanobacteria. Int. J. Mol. Sci. 20, 2789 (2019). https://doi.org/10.3390/ijms20112789

[28] Murayama, Y., Mukaiyama, A., Imai, K., Onoue, Y., Tsunoda, A., Nohara, A., et al. Tracking and visualizing the circadian ticking of the cyanobacterial clock protein kaiC in solution. EMBO J. 30, 68-78 (2011). https://doi.org/10.1038/emboj.2010.298

[29] Kabsch, W. Xds. Acta Crystallogr. D66, 125-132 (2010). https://doi.org/10.1107/S0907444909047337

[30] Yamashita, K., Hirata, K., Yamamoto, M. KAMO: Towards automated data processing for microcrystals. Acta Crystallogr. D Struct. Biol. 74, 441-449 (2018). https://doi.org/10.1107/S2059798318004576

[31] Vagin, A., Teplyakov, A. Molrep: An automated program for molecular replacement. J. Appl. Crystallogr. 30, 1022-1025 (1997). https://doi.org/10.1107/S0021889897006766

[32] Murshudov, G. N., Skubak, P., Lebedev, A. A., Pannu, N. S., Steiner, R. A., Nicholls, R. A., et al. Refmac5 for the refinement of macromolecular crystal structures. Acta Crystallogr. D Biol. Crystallogr. 67, 355-367 (2011). https://doi.org/10.1107/S0907444911001314

[33] Emsley, P., Lohkamp, B., Scott, W. G., Cowtan, K. Features and development of coot. Acta Crystallogr. D Biol. Crystallogr. 66, 486-501 (2010). https://doi.org/10.1107/S0907444910007493

[34] Swan, J. A., Sandate, C. R., Chavan, A. G., Freeberg, A. M., Etwaru, D., Ernst, D. C., et al. Coupling of distant ATpase domains in the circadian clock protein kaiC. Nat. Struct. Mol. Biol. 29, 759-766 (2022). https://doi.org/10.1038/s41594-022-00803-w